SCIENCE CHINA
Information Sciences

• RESEARCH PAPER •

November 2022, Vol. 65 212203:1–212203:18
https://doi.org/10.1007/s11432-021-3446-8

A logical network approximation to optimal control on a continuous domain and its application to HEV control

Yuhu WU[1], Jiangyan ZHANG[2*] & Tielong SHEN[3]

[1]*School of Control Science and Engineering, Dalian University of Technology, Dalian 116024, China;*
[2]*College of Mechanical and Electronic Engineering, Dalian Minzu University, Dalian 116600, China;*
[3]*Department of Engineering and Applied Sciences, Sophia University, Tokyo 102-8554, Japan*

Received 14 September 2021/Revised 14 January 2022/Accepted 12 February 2022/Published online 25 October 2022

Abstract The finite-time horizon optimal control problem is investigated for discrete-time dynamical systems defined on a continuous domain. First, the original optimal control problem in the continuous domain is approximated as one on a finite-valued domain based on a special quantification process. Under suitable assumptions, convergence analysis of the approximate optimal cost of the quantified system to the optimal cost of the original system was established with error estimation. Thereafter, the approximate problem is solved using a logical network-based method that is proposed based on the semi-tensor product of the matrix. Finally, the proposed scheme is applied to deal with the optimal control problem of a hybrid electric vehicle (HEV) powertrain system, and its effectiveness is shown by a series of simulation results.

Keywords finite horizon optimal control, logical networks, semi-tensor product, quantification, HEV control

Citation Wu Y H, Zhang J Y, Shen T L. A logical network approximation to optimal control on a continuous domain and its application to HEV control. Sci China Inf Sci, 2022, 65(11): 212203, https://doi.org/10.1007/s11432-021-3446-8

1 Introduction

In control engineering practices, numerous dynamical systems are mathematically modeled as state equations with state variables and control inputs defined in a continuous domain because the physical variables vary continuously. For example, the hybrid powertrain, which is used as a benchmark for the application of the proposed approach in this study, involves mechanical and electrical dynamics described in the continuous domain [1, 2]. For the optimal control problems of such systems, an analytical solution, even an approximate solution with satisfactory precision, is unavailable, if the state equation is represented by nonlinear functions [3, 4].

The powertrain of a hybrid electric vehicle (HEV) is a typical nonlinear system, and the energy management problems of the system have drawn significant attention because they contribute to improving energy economy and emission performance [5–8]. A notable scheme for dealing with energy management problems is to use a dynamic programming (DP) algorithm [8–10]. One of the main advantages of DP is that it provides a global optimal solution for a wide range of formulated problems. Hence, the DP algorithm has been used as a benchmark for comparison with other optimal control designs.

However, the heavy computational burden is a significant issue for practical applications of a DP solution, particularly when a nonlinear optimal control problem is considered. Generally, under the DP framework, the solution is calculated using quantitative variables of system states and control inputs, whereas the selection of quantitative factors has considerable influence on the computational burden as well as the accuracy of the optimal solution [11]. Hence, a tradeoff between the computational burden and solution accuracy is essential for the application of the DP solution. In the published studies, a few

* Corresponding author (email: zhang-jiangyan@dlnu.edu.cn)

efforts have been made to investigate the quantitative relation of the solution accuracy and computational burden [12, 13]. The work in [14] indicated that the optimal performance depends on the quantitative factor of the system state. The work in [15] introduced an updated DP algorithm and showed that the computing efficiency can be improved with non-quantitative control variables. Hence, the main purpose of this study is to deduce a quantitative analysis for the influence of solution accuracy.

Boolean networks, which can be represented by a directed graph, were originally proposed in the 1960s to simulate and analyze dynamical behaviours of genes in the gene regularity networks by Kauffman [16]. The state of each node in the Boolean network is binary (i.e., 0 or 1), indicating inactive or active, respectively. In gene regularity networks, the evolutionary dynamics of these states are governed by Boolean functions. The concept of Boolean networks can be easily extended to multiple-valued logical networks, in which the state of each node is not confined to binary. The state variable of each note in multiple-valued logical networks is restricted to a special logic domain [17], which comprises finite logic states. In recent decades, the building-up of algebraic state space representation (ASSR) approach [18] for multivalued logical systems, including Boolean networks, has precipitated a significant amount of new interest in this research area. Some fundamental and challenging issues, such as realisation, stability, observability, controllability, stabilisation, and model evolution of multiple-valued logical (or Boolean) networks, have been investigated [19–25] using the ASSR approach, and in these studies, the semi-tensor product (STP) of matrices plays an important role as a fundamental technical tool.

It has been recognized that the optimization and optimal control problems for deterministic or probabilistic multiple-valued logical networks have drawn considerable research attention and appreciation because of their extensive potential applications [26–28]. In [29], by combining the increasing dimensional technique with STP, an algebraic succinct algorithm is proposed to solve the finite horizon time optimal control problem for stochastic logical networks. Policy iteration algorithms that provide the optimal feedback law in finite iteration steps, were developed to deal with infinite time horizon optimal control problems with the average cost for deterministic and probabilistic logical networks in [30, 31], respectively. Furthermore, considerable efforts have been made to investigate a logical network-based optimal control design in a wide range of fields, such as the control of internal combustion engines [32], HEV energy management [33], and genetic regulatory networks [34].

This study considers the finite-time horizon optimal control problem for discrete-time dynamical systems on the continuous domain. Inspired by the aforementioned investigations on optimal control or optimization for multivalued logical dynamical systems, a logical network-based optimal control design approach is proposed to solve the problem defined on a continuous domain in the framework of a quantified finite domain system with an equivalent logical network expression. Note that the proposed approach can be regarded as a special discrete abstraction (quantification) method with respect to logical network expression. We refer to [35, 36] for another quantification approach, which is called control parameterisation, to the optimal control problem.

The main contributions of this study are summarized as follows. First, it is proved that the continuous dependence of optimal cost on the initial state can be guaranteed by the Lipschitz continuity of system dynamics and the cost function (including terminal cost and per-step cost function) as shown by Theorem 1. Second, the original optimal control problem defined on the continuous domain is approximated as one defined on a discrete (finite) domain by applying a special quantification process. Under suitable assumptions, the convergence of the approximate optimal cost of the quantified system to the optimal cost of the original system is established with an error estimate, as shown by Theorem 2. Thereafter, based on STP, an algorithm (Algorithm 1) was presented to solve the counterpart approximate optimal control problem. Finally, the effectiveness of the proposed algorithm was evaluated using a numerical example and an application to solve the HEV energy management problem.

The remainder of this paper is organized as follows. Section 2 introduces the problem formulation, including the corresponding essential notations and concepts. Section 3 presents the main results. After the convergence analysis and error estimation of the approximate optimal cost of the quantified system, the corresponding logical network-based DP algorithm is presented. In Section 4, the application of the proposed control approach to the HEV energy management problem is discussed. Finally, the conclusion is presented in Section 5. A preliminary version of this work was partially presented in [37].

2 Control problem formulation

Consider the following discrete-time dynamical system:

$$x(t+1) = f(x(t), u(t)), \tag{1}$$

where $x \in X \subset \mathbb{R}^{N_x}$ and $u \in U \subset \mathbb{R}^{N_u}$ are the state and control vectors, respectively, and $f : X \times U \to X$ is the given function. Assume that X is a compact and convex subset of $\mathbb{R}^{N_x}$, and U is also a compact and convex subset of $\mathbb{R}^{N_u}$. The initial condition for the system (1) is

$$x(0) = x_0 \in X. \tag{2}$$

Let $\boldsymbol{u}$, known as an admissible control input, denote a control sequence $\{u(t) : t = 0, \ldots, T-1\}$ in U, and $\mathcal{U}$ be the class of all admissible controls. Let $x(t; f, x_0, \boldsymbol{u}), t \geqslant 0$ denote the solution of the dynamical system (1) with the initial state (2) and corresponding to the control inputs $\boldsymbol{u} \in \mathcal{U}$. If no confusion may arise, the solution $x(t; f, x_0, \boldsymbol{u})$ is abbreviated as $x(t)$ for notational convenience.

Given an initial state $x_0 \in X$ and an admissible control $\boldsymbol{u} = \{u(t)\}_{t=0}^{T-1} \in \mathcal{U}$, consider the finite horizon cost functional

$$J(f, x_0, \boldsymbol{u}) = h(x(T)) + \sum_{t=0}^{T-1} g(x(t), u(t)) \tag{3}$$

subject to the system equation constraint (1), where the terminal cost $h : X \to \mathbb{R}$ and the per-step cost $g : X \times U \to \mathbb{R}$ are given real-valued functions.

The following conditions are assumed throughout:

(C1) Assume that f is joint Lipschitz continuous on $X \times U$ in the following sense:

$$|f(x, u) - f(y, v)| \leqslant k_f \left(|x - y| + |u - v|\right), \tag{4}$$

for all $x, y \in X$, and $u, v \in U$, with Lipschitz constant $k_f > 0$, where $|\cdot|$ denotes the 2-norm of the finite-dimensional vector.

(C2) Assume that h is Lipschitz continuous on X, and g is joint Lipschitz continuous on $X \times U$. In other words, $k_h > 0$ and $k_g > 0$ exist such that $\forall\ x, y \in X$ and $u, v \in U$,

$$|h(x) - h(y)| \leqslant k_h |x - y|, \tag{5}$$

$$|g(x, u) - g(y, v)| \leqslant k_g \left(|x - y| + |u - v|\right). \tag{6}$$

The optimal cost function $J^*(f, x_0)$ is defined as

$$J^*(f, x_0) = \inf_{\boldsymbol{u} \in \mathcal{U}} J(f, x_0, \boldsymbol{u}). \tag{7}$$

Then the considered finite horizon optimal control problem can be formulated as follows.

Problem (P). Consider the discrete dynamical system (1) with initial state (2). Determine an optimal control input $\boldsymbol{u}_{f,x_0} \in \mathcal{U}$ that guarantees the cost functional $J(f, x_0, \boldsymbol{u}_{f,x_0})$ to reach the optimal cost $J^*(f, x_0)$, that is

$$J(f, x_0, \boldsymbol{u}_{f,x_0}) = J^*(f, x_0).$$

3 Logical network-based approximate optimal control

In this section, we first provide a continuous dependence result of the optimal performance $J^*(f, x_0)$ under the initial condition x_0 and assumptions (C1) and (C2). Subsequently, by introducing a special portion pair given by Definition 1, a quantitative approximate process of problem (P) is presented with convergence analysis. Finally, a logical network-version of the DP algorithm is proposed to solve the quantitative approximate optimal control problem.

3.1 Continuous dependence of optimal cost on initial state

Lemma 1. Under assumptions (C1) and (C2), the trajectory $x(t; f, x_0, \boldsymbol{u})$ and the cost functional $J(f, x_0, \boldsymbol{u})$ are Lipschitz continuous in $X \times \mathcal{U}$. Specifically, for any $x_0, y_0 \in X$ and $\boldsymbol{u} = \{u(t)\}_{t=0}^{T-1}, \boldsymbol{v} = \{v(t)\}_{t=0}^{T-1} \in \mathcal{U}$,

$$|x(t; f, x_0, \boldsymbol{u}) - x(t; f, y_0, \boldsymbol{v})| \leqslant k_f^t |x_0 - y_0| + K_1(t)\|\boldsymbol{u} - \boldsymbol{v}\|, \tag{8}$$

$$|J(f, x_0, \boldsymbol{u}) - J(f, y_0, \boldsymbol{v})| \leqslant K_2|x_0 - y_0| + K_3\|\boldsymbol{u} - \boldsymbol{v}\|, \tag{9}$$

with

$$K_1(t) = \frac{k_f - k_f^{t+1}}{1 - k_f}, \quad K_2 = k_h k_f^T + k_g K_1(T-1), \quad K_3 = k_h K_1(T) + k_g \frac{(T-1)k_f - Tk_f^2 + k_f^{T+1}}{(1-k_f)^2}, \tag{10}$$

where the norm $\|\boldsymbol{u}\|$ on $\mathcal{U}$ is defined as

$$\|\boldsymbol{u}\| = \max\{|u(t)| : 0 \leqslant t \leqslant T-1\}. \tag{11}$$

Proof. Refer to Appendix A.

We now give the continuous dependence of optimal cost J^* on an initial condition.

Theorem 1. Under assumptions (C1) and (C2), the optimal cost $J^*(f, x_0)$ is Lipschitz continuous in X, that is, for any $x_0, y_0 \in X$,

$$|J^*(f, x_0) - J^*(f, y_0)| \leqslant K_2|x_0 - y_0|, \tag{12}$$

where K_2 is given by (10) in Lemma 1.

Proof. Refer to Appendix A.

3.2 Quantification process

Definition 1. Let $\{\mathscr{S}_n\}_{n=1}^{\infty}$ be a collection of finite partitions of X with $\mathscr{S}_n = \{S_n^i\}_{i=1}^{\Upsilon_n}$, and $\{\mathscr{X}_n\}_{n=1}^{\infty}$ be a collection of finite points of X with $\mathscr{X}_n = \{x_n^i\}_{i=1}^{\Upsilon_n}$. We call $\{\mathscr{S}_n, \mathscr{X}_n\}_{n=1}^{\infty}$ a set of partition pair with a density (SPPD) of X if for each $n \geqslant 1$, $\mathscr{S}_n$ and $\mathscr{X}_n$ satisfy the following conditions:

(B1) $S_n^i \cap S_n^j = \emptyset, i \neq j;\ \bigcup_{i=1}^{\Upsilon_n} S_n^i = X$;

(B2) $x_n^i \in S_n^i, \forall i = 1, \ldots, \Upsilon_n$;

(B3) $\lim_{n\to\infty} \mathscr{X}_n$ is dense in X, which is equivalent to requiring that

$$\lim_{n\to\infty} d_{\mathrm{H}}(\mathscr{X}_n, X) = 0, \tag{13}$$

where $d_{\mathrm{H}}(\mathscr{X}_n, X)$ is the Hausdorff distance of $\mathscr{X}_n$ and X, and the Hausdorff distance $d_{\mathrm{H}}(Y, X)$ of two nonempty subsets $Y, X \in \mathbb{R}^n$ is defined as

$$d_{\mathrm{H}}(Y, X) = \max\left\{\sup_{y\in Y}\inf_{x\in X}|x-y|,\ \sup_{x\in X}\inf_{y\in Y}|y-x|\right\}.$$

Definition 2. For any partition collection $\mathscr{S}_n = \{S_n^i\}_{i=1}^{\Upsilon_n}$ of X, the maximum volume of $\mathscr{S}_n$, denoted by $\|\mathscr{S}_n\|$, is defined as

$$\|\mathscr{S}_n\| = \max_{1\leqslant i\leqslant \Upsilon_n} \sup\left\{|x-y| : x, y \in S_n^i\right\}. \tag{14}$$

Note that condition (B2) in Definition 1 implies that for given $\mathscr{S}_n$ and $\mathscr{X}_n$, with $n \geqslant 0$, point x_n^i can be regard as a representative point of partition S_n^i $(i = 1, \ldots, \Upsilon_n)$. Furthermore, we have the following simple facts.

Proposition 1. In Definition 1, from condition (B2), condition (B3) is equivalent to the following condition:

$$\lim_{n\to\infty} \|\mathscr{S}_n\| = 0. \tag{15}$$

Example 1. Let $X=[a,b]$ be a closed interval in $\mathbb{R}^1$ with $a<b$. For any integer $N>0$, we define a finite sequence $\{a_n^i, 0\leqslant i\leqslant \Upsilon_n\}$ with $\Upsilon_n=2^n$ as follows:

$$a_n^i = a + ic_n,\quad i=0,1,\ldots,2^n, \tag{16}$$

where c_n is defined as $c_n=(b-a)/2^n$. Note that $a_n^0=a$ and $a_n^{2^n}=b$ according to the definition of $\{a_n^i\}$ given by (16). Thereafter, for each $n>0$, set the subdivisions $\mathscr{A}_n=\{A_n^i\}_{i=1}^{2^n}$ of the considered interval $X=[a,b]$ as

$$\begin{cases} A_n^1=[a_n^0,a_n^1], \text{ and}\\ A_n^i=(a_n^{i-1},a_n^i],\ i=2,\ldots,2^n. \end{cases} \tag{17}$$

These subdivisions of X are pairwise disjoint, i.e.,

$$A_n^i\cap A_n^j=\emptyset,\ 1\leqslant i,j\leqslant 2^n,\ i\neq j,\quad\text{and}\quad \bigcup_{i=1}^{2^n} A_n^i=[a,b].$$

Hence, $\{\mathscr{A}_n\}_{n=1}^{\infty}$ satisfies condition (B1) of Definition 1. Additionally, we set $\mathscr{X}_n=\{a_n^i\}_{i=1}^{2^n}$. Then, $\lim_{n\to\infty} d_{\rm H}(\mathscr{X}_n,[a,b])=0$. Hence, $\{\mathscr{A}_n,\mathscr{X}_n\}_{n=1}^{\infty}$ is an SPPD of $[a,b]$.

Definition 3. For a given SPPD $\{\mathscr{S}_n,\mathscr{X}_n\}_{n=1}^{\infty}$ of X with subdivisions $\mathscr{S}_n=\{S_n^i\}_{i=1}^{\Upsilon_n}$ and finite points $\mathscr{X}_n=\{x_n^i\}_{i=1}^{\Upsilon_n}$, we define the simple functions $q_n: X\to\mathscr{X}_n$, $n\geqslant 1$ as follows:

$$q_n(z)=\sum_{i=1}^{\Upsilon_n} x_n^i \mathbb{1}_{S_n^i}(z),\quad \forall z\in X. \tag{18}$$

Here, the characteristic function of the subset $S_n^i\subset X$ denoted by $\mathbb{1}_{S_n^i}$ is defined as follows:

$$\mathbb{1}_{S_n^i}(z)=\begin{cases} 1,\ z\in S_n^i,\\ 0,\ z\notin S_n^i. \end{cases}$$

According to the definition of $q_n(\cdot)$, we have

$$|q_n(z)-z|\leqslant \|\mathscr{S}_n\|,\quad \forall z\in X. \tag{19}$$

In fact, under the condition (B1) of Definition 1, there exists a unique $i_0\in\{1,\ldots,\Upsilon_n\}$ such that $z\in S_n^{i_0}$. Then, we have

$$|q_n(z)-z|=|x_n^i-z|\leqslant \sup_{z,w\in S_n^{i_0}}|z-w|\leqslant \|\mathscr{S}_n\|.$$

Assume that for all $m\geqslant 1$, $\{\mathscr{E}_m,\mathscr{U}_m\}_{m=1}^{\infty}$ is an SPPD of U, with $\mathscr{E}_m=\{E_m^i\}_{i=1}^{\Upsilon_m}$ and $\mathscr{U}_m=\{u_m^i\}_{i=1}^{\Upsilon_m}$. Thus, $\{\mathscr{E}_m,\mathscr{U}_m\}_{m=1}^{\infty}$ satisfies the conditions given by Definition 1 for the control set U.

Definition 4. Assume that $\{\mathscr{S}_n,\mathscr{X}_n\}_{n=1}^{\infty}$ is an SPPD of X and $\{\mathscr{E}_m,\mathscr{U}_m\}_{m=1}^{\infty}$ denotes the SPPD of U. For operator f with respect to the discrete-time dynamical system (1), we define the quantification operator $\hat{f}_m^n: X\times U\to\mathscr{X}_n$ as

$$\hat{f}_m^n(x,u)=q_n\big(f(x,q_m(u))\big),\quad \forall x\in X,\ u\in U. \tag{20}$$

The following proposition expresses the approximation relationship between the quantification operator $\hat{f}_n^m$ and original operator $f: X\times U\to X$.

Proposition 2. For any $n\geqslant 1$ and $m\geqslant 1$, the quantification operator $\hat{f}_m^n$ satisfies the following property:

$$\left|\hat{f}_m^n(x,u)-f(x,u)\right|\leqslant \|\mathscr{S}_n\|+k_f\|\mathscr{E}_m\|, \tag{21}$$

for any $x\in X$ and $u\in U$, where $\|\mathscr{S}_n\|$ and $\|\mathscr{E}_m\|$ are the maximum volumes of $\mathscr{S}_n$ and $\mathscr{E}_m$, respectively, as defined in (14).

Proof. Refer to Appendix A.

Given an SPPD $\{\mathscr{S}_n, \mathscr{X}_n\}_{n=1}^{\infty}$ of X and an SPPD $\{\mathscr{E}_m, \mathscr{U}_m\}_{m=1}^{\infty}$ of U, consider the following quantified system:

$$\begin{cases} \hat{x}_n(t+1) = \hat{f}_m^n(\hat{x}_n(t), u(t)), \\ \hat{x}_n(0) = q_n(x(0)). \end{cases} \tag{22}$$

Let $\hat{x}(t; \hat{f}_m^n, x_0, \boldsymbol{u}), t \geqslant 0$ denote the solution of the quantified dynamical system (22) with the initial state (2) and the corresponding control inputs $\boldsymbol{u} \in \mathcal{U}$. If no confusion may arise, the solution $\hat{x}(t; \hat{f}_m^n, x_0, \boldsymbol{u})$ is abbreviated as $\hat{x}(t)$ for notational convenience. Let $\boldsymbol{u}_m$ denote the control sequence $\{u_m(t) : 0 \leqslant t \leqslant T-1\}$, where $u_m(t) \in \mathscr{U}_m = \{u_m^i\}_{i=1}^{\Upsilon_m}$ for all $t \geqslant 0$. Let $\mathcal{U}_m$ be the class of all such admissible controls.

Based on the above quantification process, we define the approximate optimal control problem $(\mathrm{AP})_m^n$ as follows.

Problem $(\mathrm{AP})_m^n$. For a quantified dynamical system defined by (22), with the initial state (2), determine an optimal control sequence $\boldsymbol{u}_{f_m^n, x_0} \in \mathcal{U}_m$ such that its corresponding cost functional $J(\hat{f}_m^n, x_0, \boldsymbol{u}_{\hat{f}_m^n, x_0})$ reaches the optimal cost:

$$J^*(\hat{f}_m^n, x_0) = \inf_{\boldsymbol{u}_m \in \mathcal{U}_m} J(\hat{f}_m^n, x_0, \boldsymbol{u}_m). \tag{23}$$

Lemma 2. The solution of the quantified systems (22) satisfies the following condition:

$$|\hat{x}_n(t) - x(t)| \leqslant (K_1(t+1)/k_f)\|\mathscr{S}_n\| + K_1(t)\|\mathscr{E}_m\|, \tag{24}$$

where $\hat{x}(t)$ and $x(t)$ are abbreviations of $\hat{x}(t; \hat{f}_m^n, x_0, \boldsymbol{u}), t \geqslant 0$ and $x(t; f, x_0, \boldsymbol{u}), t \geqslant 0$, respectively. $K_1(\cdot)$ is defined by (10).

Proof. Refer to Appendix A.

Lemma 3. For a given admissible control input $\boldsymbol{u} \in \mathcal{U}$ with initial condition (2), we obtain the following estimation:

$$|J(f, x_0, \boldsymbol{u}) - J(\hat{f}_m^n, x_0, \boldsymbol{u})| \leqslant K_4\|\mathscr{S}_n\| + K_5\|\mathscr{E}_m\|, \tag{25}$$

with $K_4 = (k_h K_1(T+1) + k_g \sum_{t=1}^{T-1} K_1(t+1))/k_f$, and $K_5 = k_g K_1(T+1) + k_h \sum_{t=1}^{T-1} K_1(t+1)$. Especially, when $\boldsymbol{u} \in \mathcal{U}_m$, we have

$$|J(f, x_0, \boldsymbol{u}) - J(\hat{f}_m^n, x_0, \boldsymbol{u})| \leqslant K_4\|\mathscr{S}_n\|. \tag{26}$$

Proof. Refer to Appendix A.

Finally, the convergence result of the approximate optimal cost given by (23) with respect to the quantified system (22) to the optimal cost of the original systems (1) is given by the following theorem.

Theorem 2. Suppose that with $m \geqslant 1$ and $n \geqslant 1$, $\boldsymbol{u}_{f,x_0}$ and $\boldsymbol{u}_{\hat{f}_m^n, x_0}$ are the optimal controls of the original problem (P) and the approximate problem $(\mathrm{AP})_m^n$, respectively. Then,

$$\lim_{n\to\infty, m\to\infty} J(\hat{f}_m^n, x(0), \boldsymbol{u}_{\hat{f}_m^n, x_0}) = J(f, x(0), \boldsymbol{u}_{f,x_0}). \tag{27}$$

More precisely,

$$|J^*(\hat{f}_m^n, x_0) - J^*(f, x_0)| \leqslant (K_2 + K_4)\|\mathscr{S}_n\| + (K_3 + K_5)\|\mathscr{E}_m\|. \tag{28}$$

Proof. Refer to Appendix A.

Remark 1. The error estimation given by (28) in Theorem 2 implies that the error bound of $|J^*(\hat{f}_m^n, x_0) - J^*(f, x_0)|$ depends on the quantification levels $\|\mathscr{S}_n\|$ and $\|\mathscr{E}_m\|$, with respect to the states and control inputs.

3.3 Main results on solving the approximate problem

In this subsection, a multiple-logical network equivalent expression given by (22) for the finite-domain approximate system is first deduced, and then a new DP algorithm deduced based on a logical network is proposed to solve the counterpart approximate optimal control problem $(\mathrm{AP})_m^n$.

It is essential to introduce the following notations and definitions in the subsequent sections of this paper. Let $\Delta_N := \{\delta_N^i | i = 1, \ldots, N\}$ with δ_N^i representing the i-column of an N-dimensional identity matrix I_N.

If the columns of a given matrix $E \in \mathbb{R}^{M\times N}$ satisfy $\mathrm{Col}(E) \subset \Delta_M$, then matrix E is called a logical matrix, which implies that the matrix E has the characteristic that $E = [\delta_M^{i_1}, \delta_M^{i_2}, \ldots, \delta_M^{i_N}]$ and can be briefly defined as $E = \delta_M[i_1, i_2, \ldots, i_N]$. The set of $M \times N$ logical matrices is defined as $\mathcal{L}_{M\times N}$. For the given positive integers n and p, let $s = \mathrm{lcm}\{n, p\}$ be the least common multiple of n and p. For any $E \in \mathbb{R}^{m\times n}$ and $F \in \mathbb{R}^{p\times q}$, the STP of E and F is defined as follows [38]:

$$E \ltimes F := (E \otimes I_{s/n})(F \otimes I_{s/p}), \tag{29}$$

where $\otimes$ denotes the Kronecker product.

To use the multiple logical expression, we identify the subset $\mathscr{X}_n = \{x_n^i\}_{i=1}^{\Upsilon_n}$ with $\Delta_{\Upsilon_n} = \{\delta_{\Upsilon_n}^i\}_{i=1}^{\Upsilon_n}$ as follows:

$$x_n^i \sim \delta_{\Upsilon_n}^i, \quad i = 1, 2, \ldots, \Upsilon_n.$$

Under this identification, each element x of $\mathscr{X}_n$ corresponds to a vector form of x in Δ_{Υ_n}. Similarly, the control set $\mathcal{U}_m$ can be identified as Δ_{Υ_m} by the following:

$$u_m^j \sim \delta_{\Upsilon_m}^j, \quad j = 1, 2, \ldots, \Upsilon_m.$$

Furthermore, the logical function can be converted into an algebraic formalization based on the STP, as given in the following lemma.

Lemma 4 (Theorem 3.2 of [38])**.** Let $f : \mathcal{D}^p \to \mathcal{D}^q$ be a logical function. Set $y = f(x_1, x_2, \ldots, x_p) \in \mathcal{D}^q$ with $(x_1, x_2, \ldots, x_p) \in \mathcal{D}^p$. Then the logical function f can be rewritten in a multiple linear form as

$$f(x_1, x_2, \ldots, x_n) = M_f \ltimes_{i=1}^n x_i, \tag{30}$$

where $M_f \in \mathcal{L}_{2^q\times 2^p}$, which is called the structure matrix of logical function f, and is a logical matrix uniquely determined by f. Eq. (30) is called the algebraic formalization of logical function f.

Under the above logical vector setting, it is easily observed that if the quantification operator $\hat{f}_m^n$ defined in (20) is restricted on $\mathcal{X}_n \times \mathcal{U}_m$, then it can be regarded as a logical operator from the product logical space $\Delta_{\Upsilon_n} \ltimes \Delta_{\Upsilon_m}$ to logical space Δ_{Υ_m}. As a result, by applying Lemma 4, the algebraic equivalent expression of quantified systems (22) is given by the following proposition.

Proposition 3. For any given $n \in N$ and $m \in N$, the quantification dynamics $\hat{f}_m^n : \Delta_{\Upsilon_n} \ltimes \Delta_{\Upsilon_m} \to \Delta_{\Upsilon_n}$ formulated by (22) can be rewritten as linear multiple-valued logical dynamics, as follows:

$$\hat{x}_n(t+1) = \hat{L}_m^n \ltimes \hat{u}_m(t) \ltimes \hat{x}_n(t), \tag{31}$$

where the logical matrix $\hat{L}_m^n \in \mathcal{L}_{\Upsilon_n\times\Upsilon_m}$ is uniquely determined by $\hat{f}_m^n$.

It is also noticed that if the terminal cost h and the per-step cost function g are restricted to $\mathcal{X}_n$ and $\mathcal{X}_n \times \mathcal{U}_m$, respectively, then under the above identification, the cost function can be represented as follows:

$$h(x) = x^\top H, \quad \forall x \in \Delta_{\Upsilon_n},$$
$$g(x, u) = x^\top G u, \quad \forall x \in \Delta_{\Upsilon_n},\ u \in \Delta_{\Upsilon_m},$$

where $H = (H_i)_{\Upsilon_m}$ with $H_i = h(\delta_{\Upsilon_n}^i)$, and $G = (G_{i,j})_{\Upsilon_n\times\Upsilon_m}$ with $G_{i,j} = g(\delta_s^i, \delta_r^j)$. As a result, for any initial state, $x_0 \in \Delta_{\Upsilon_n}$, the objective function (3) can be rewritten by

$$J(f, x_0, \boldsymbol{u}) = x(T)^\top H + \sum_{t=0}^{T-1} x(t)^\top G u.$$

Under the framework of a multiple-valued logical network, the following DP-based algorithm was proposed to solve the counterpart problem $(\mathrm{AP})_m^n$.

Remark 2. Note that Algorithm 1 is the deterministic version of the DP algorithm proposed in [29] for solving the finite time optimization problem for the stochastic multiple-valued logical dynamical systems.

Algorithm 1 Logical-network based algorithm for counterpart problem $(\mathrm{AP})_m^n$

Initialization:

(1) Calculate the structure matrix $\hat{L}_m^n$, terminal cost vector H, and per-stage cost matrix G;

(2) Set $s = \Upsilon_n$, $r = \Upsilon_m$, $V_l^* = H$, and $l = 0$;

Step A:

Solve

$$V_{l+1}^* = \begin{pmatrix} \min\limits_{j=1,\ldots,r} \left\{G_{1j} + (\delta_s^1)^\top \ltimes (\delta_r^j)^\top \hat{L}_m^n V_l^*\right\} \\ \vdots \\ \min\limits_{j=1,\ldots,r} \left\{G_{sj} + (\delta_s^s)^\top \ltimes (\delta_r^j)^\top \hat{L}_m^n V_l^*\right\} \end{pmatrix},$$

and obtain the corresponding optimal control feedback matrix:

$$\Phi_{T-l+1}^* = L_r[q_1, \ldots, q_s], \text{ where for } i = 1, \ldots, s,$$
$$q_i = \arg \min_{j=1,\ldots,r} \left\{G_{ij} + (\delta_s^i)^\top \ltimes (\delta_r^j)^\top \mathbb{P}\mathcal{K}\right\};$$

Update $l = l + 1$.

Step B:

(1) If $l < T$, then go to Step A;

(2) If $l = T$, then go to Step B(3);

(3) If $x_0 \in S_n^i$, then $J(\hat{f}_m^n, x_0) = (\delta_s^i)^\top V_{T-1}^*$ and stop.

3.4 Numerical example

Consider a linear dynamical system:

$$x(t+1) = Ax(t) + Bu(t), \tag{32}$$

with $x \in \mathbb{R}^2$ and $u \in \mathbb{R}$, respectively. For system (32), we intend to minimise the finite-horizon linear quadratic regulator problem as follows:

$$\min_{u(t)} J = h(x(T)) + \sum_{t=0}^{T-1} g(x(t), u(t)), \tag{33}$$

with $h(x) = x^\top Px$, $g(x, u) = x^\top Qx + u^\top Ru$. Set $R = 10$, and

$$A = \begin{bmatrix} 0.25 & 2 \\ 1 & 0.1 \end{bmatrix}, \quad B = \begin{bmatrix} 0 \\ 1.5 \end{bmatrix}, \quad P = \begin{bmatrix} 2 & 1 \\ 1 & 2 \end{bmatrix}, \quad Q = \begin{bmatrix} 5 & 2 \\ 2 & 1 \end{bmatrix}.$$

Without control constraints, according to the Bellman principle-based recursive functional equation [39], the exact (analytical) optimal solution of problem (33) can be solved by using the following recursive equations, that is, for each $t = T-1, \ldots, 0$,

$$J^*(x_0) = V_{T-1}^*(x(0)), \tag{34a}$$
$$u^*(t) = C_{T-1-t}x(t), \tag{34b}$$
$$V_{T-1-t}^*(x(t)) = x(t)^\top D_{T-1-t}x(t), \tag{34c}$$
$$C_t = -(B^\top D_{t-1}B + R)^{-1}B^\top D_{t-1}A, \tag{34d}$$
$$D_t = Q + C_t^\top RC_t + (A + BC_t)^\top D_{t-1}(A + BC_t), \tag{34e}$$
$$C_0 = -(B^\top PB + R)^{-1}B^\top PA, \tag{34f}$$
$$D_0 = Q + C_0^\top RC_0 + (A + BC_0)^\top(A + BC_0). \tag{34g}$$

We set $T = 30$, $X = [-1, 3] \times [-1, 1] \subset \mathbb{R}^2$, and $U = [-2, 1] \subset \mathbb{R}^1$. Let the initial condition be $x_0 = [1, 1]^\top$. Then, it is easy to verify that the optimal control law $u^*(t)$ without any constraint and the corresponding optimal solution $x^*(t)$ obtained from (34) satisfy $(x^*(t)) \in X$ and $u^*(t) \in U$, respectively. This implies that $u^*(t), 0 \leqslant t \leqslant T-1$ obtained from (34) is also the optimal control input with constraint $u(t) \in U$.

Based on the analytical solution, a quantitative analysis can be performed to evaluate the approximate optimal solution obtained by the logical network-based Algorithm 1. An approximate solution $\hat{x}^*(t)$ of

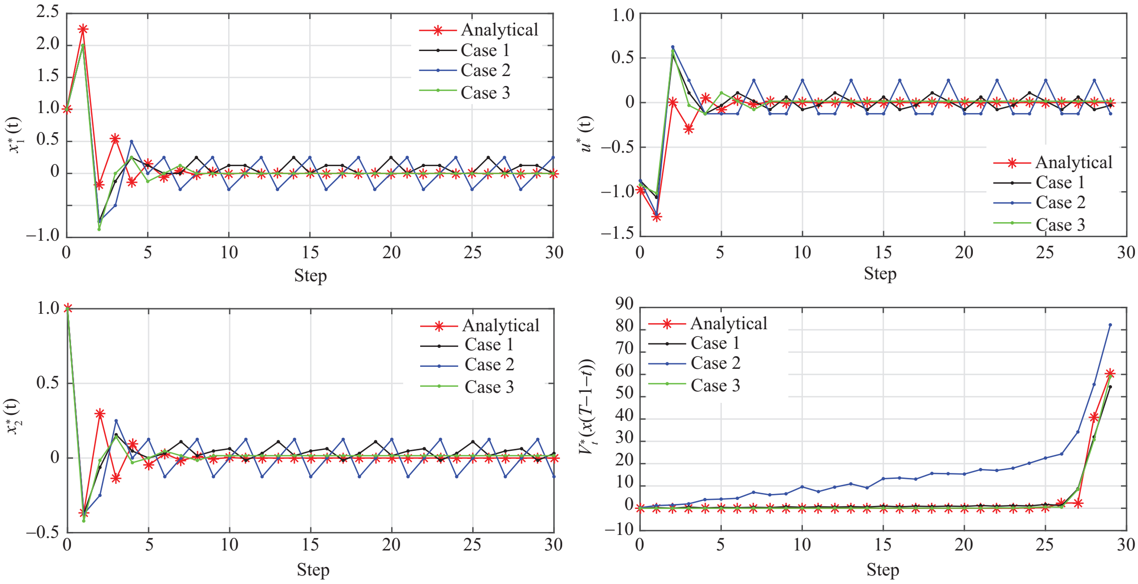

Figure 1 (Color online) Logical network-based approximate solutions vs. analytical solution.

the corresponding logical system was generated. Let the quantification indices for the states and control variable be n_{xi} $(i = 1, 2)$ and n_u. The quantification finite sequences of the states and control variable are as follows:

$$\hat{x}_{in}^l = x_{i\min} + lc_{xin},\ l = 0, 1, \ldots, 2^{n_{xi}} \quad \text{with} \quad c_{xin} = \frac{x_{i\max} - x_{i\min}}{2^{n_{xi}}}, \tag{35a}$$

$$u^l = u_{\min} + lc_{un},\ l = 0, 1, \ldots, 2^{n_u} \quad \text{with} \quad c_{un} = \frac{u_{\max} - u_{\min}}{2^{n_u}}, \tag{35b}$$

and the corresponding equidistance partitions of the state domain X and control domain U are similar to (17) of Example 1. With the above quantification process (35) and according to Definition 4, we obtain the following corresponding quantified system:

$$\begin{cases} \hat{x}^l(t+1) = q_n(A\hat{x}^l(t) + Bu^l(t)), \\ \hat{x}^l(0) = q_n(x(0)). \end{cases} \tag{36}$$

Furthermore, to evaluate the logical network-based strategy, three approximate solutions were deduced by taking diverse quantification indices for the states and control variables. Specifically,

Case 1: $n_{x1} = 5$, $n_{x2} = 5$ and $n_u = 6$;

Case 2: $n_{x1} = 8$, $n_{x2} = 5$ and $n_u = 3$;

Case 3: $n_{x1} = 8$, $n_{x2} = 5$ and $n_u = 6$.

Finally, three approximate solutions of problem (33) with respect to the quantified system (36) are obtained by applying Algorithm 1.

The analytical solutions obtained using (34) with the three approximate solutions are shown in Figure 1 and Table 1 where the variances of the two states and the control variable are given. As shown in Figure 1, the three approximate solutions of the quantified system converged to the analytical solution with acceptable precision. Moreover, it can be observed from the curves shown in Figure 1 and the data in Table 1 that bigger quantification indices can lead to more exact solution, and this observation confirms the result (28) of Theorem 2; however, much computation time is consumed. Hence, in practical applications, the tread-off between precision and computation time must be considered according to Remark 1 given for Theorem 2.

4 HEV energy management application

In this section, an application of the proposed control strategy to deal with the energy management of the HEV powertrain system is presented. The considered HEV had a parallel structure, as shown in Figure 2.

Table 1 Exact solutions x_i^* $(i = 1, 2, 3)$ and u^* vs. corresponding values solved by the logical control strategy

Case	Variance			Computation
	$\frac{1}{T}\sum_{t=1}^{T}(\hat{x}_1^{l*}(t) - x_1^*(t))^2$	$\frac{1}{T}\sum_{t=1}^{T}(\hat{x}_2^{l*}(t) - x_2^*(t))^2$	$\frac{1}{T}\sum_{t=1}^{T}(\hat{u}^{l*}(t) - u^*(t))^2$	time (s)
Case 1	0.047	0.010	0.022	13.13
Case 2	0.101	0.025	0.050	21.065
Case 3	0.037	0.007	0.018	108.879

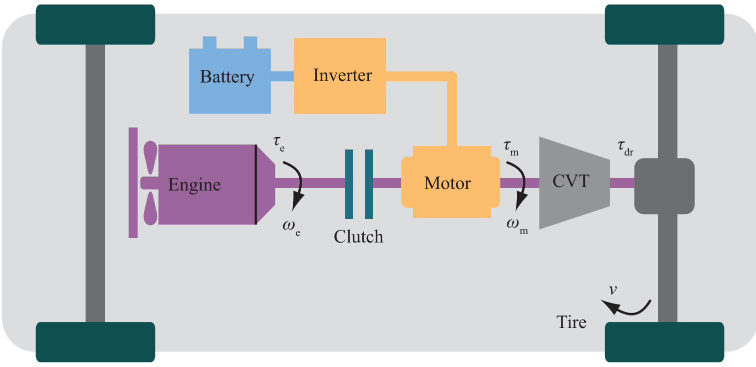

Figure 2 (Color online) A parallel HEV.

The powertrain system consisted of an internal combustion engine and an electric motor connected by a clutch. This implies that the engine can be cut off from the drivetrain. The driving power from the power sources is transferred to the driving shaft through a constantly variable transmission (CVT) system. Let v and $\tau_{\rm dr}$ denote the speed and driving torque demands of the vehicle, respectively. Energy management distributes the power demand $P_{\rm dr}(= \tau_{\rm dr}v)$ between the two power sources. The following system models were used to formulate the energy management problem.

To solve the power distribution problem using an optimal control scheme, the following physical relations of the system were introduced. Let $i_{\rm g}$ denote the gear ratio of the CVT system, i_0 denote the final differential gear ratio, and η_f denote the transmission efficiency. According to the physics of the mechanical transmission system shown in Figure 2, the driving torque $\tau_{\rm dr}$ is related to the engine torque $\tau_{\rm e}$ and motor torque $\tau_{\rm m}$ by the following equation:

$$\tau_{\rm dr} = i_{\rm g}i_0\eta_f(\tau_{\rm e} + \tau_{\rm m}). \tag{37}$$

Moreover, the engine speed $\omega_{\rm e}$ and the motor speed $\omega_{\rm m}$ are related to the vehicle wheel speed v, as follows:

$$\begin{cases} \omega_{\rm e} = 0,\ \omega_{\rm m} = i_{\rm g}i_0\dfrac{1}{R_{\rm tire}}v, & \text{clutch is disengaged,} \\ \omega_{\rm e} = \omega_{\rm m} = i_{\rm g}i_0\dfrac{1}{R_{\rm tire}}v, & \text{clutch is engaged,} \end{cases} \tag{38}$$

where $R_{\rm tire}$ denotes the wheel radius.

Let M, g, and θ denote the vehicle mass, gravitational acceleration, and road slop, respectively. Moreover, regarding the vehicle, let $\mu_{\rm r}$ denote the coefficient of the rolling resistance, A denote the frontal area, and $\rho_{\rm a}$ and $C_{\rm d}$ denote the air density and drag coefficient, respectively. The road load force $F(v)$ on the vehicle can be represented by

$$F(v) = Mg(\mu_{\rm r}\cos\theta + \sin\theta) + \frac{1}{2}\rho_{\rm a}AC_{\rm d}v^2. \tag{39}$$

In this study, suppose that the road slop is neglected, that is, $\theta = 0$. According to Newton's second law, the longitudinal motion of a vehicle can be represented by the following dynamics:

$$M\dot{v} = \frac{\tau_{\rm dr}}{R_{\rm tire}} - F(v). \tag{40}$$

Furthermore, to design a logical network-based control law, the acceleration $\dot{v}$ is approximated to a difference equation, that is,

$$\dot{v}(t) = \Delta v(t_k) = \frac{v(t_{k+1}) - v(t_k)}{\Delta t}, \tag{41}$$

where t_k $(k = 0, 1, \ldots)$ denotes the sampling time and Δt denotes the sampling period. Then, regarding the desired vehicle speed trajectory $v^*(t_k)$, combining relations (39), (40), and (41) shows that the driving torque demand $\tau^*_{\rm dr}(t_k)$ satisfies the following equation:

$$\tau^*_{\rm dr}(t_k) = R_{\rm tire}\Big[M \cdot \Delta v(t_k) + \mu_{\rm r} Mg + \frac{1}{2}\rho_{\rm a} AC_{\rm d} v^2(t_k)\Big]. \tag{42}$$

Finally, the electrical power supplied to the motor is from the vehicle battery that has maximum charge capacity $Q_{\rm b}$; that is, the electrical energy is limited during the vehicle operating stage. The system for electrical energy flow in an HEV can be represented as an open-circuit voltage source. Let $R_{\rm b}$ and $U_{\rm o}$ denote the internal resistance and open-circuit voltage of an electrical system, respectively. The evolution dynamics of the electrical energy can be formulated as the following differential equation in terms of the battery state of charge (SOC):

$$\begin{aligned} \dot{\rm SOC}(t) &= f\big({\rm SOC}(t), \tau_{\rm m}(t), \omega_{\rm m}(t)\big) \\ &= \frac{-U_{\rm o} + \sqrt{U_{\rm o}^2 - 4R_{\rm b}\big[\tau_{\rm m}(t)\omega_{\rm m}(t) - P_{\rm m}^{\rm loss}(\tau_{\rm m}(t), \omega_{\rm m}(t))\big]}}{2Q_{\rm b}R_{\rm b}}. \end{aligned} \tag{43}$$

Furthermore, to realize a logical network-based control design, the above differential equation is approximated to be a difference one, that is,

$${\rm SOC}(t_{k+1}) = {\rm SOC}(t_k) + \Delta t \cdot f\big({\rm SOC}(t_k), \tau_{\rm m}(t_k), \omega_{\rm m}(t_k)\big). \tag{44}$$

In (43), $P_{\rm m}^{\rm loss}$ represents the power losses of the motor and is depended on the motor operating points. For the control design, a polynomial model was identified for $P_{\rm m}^{\rm loss}$ using experimental data.

4.1 Energy management problem

To achieve the desired vehicle trajectory v^*, the engine torque demand $\tau^*_{\rm e}$, motor torque demand $\tau^*_{\rm m}$, and desired gear ratio $i^*_{\rm g}$ should be determined by the control strategy. In other words, the objective of energy management is to determine the operating points $(\omega^*_{\rm e},\ \tau^*_{\rm e})$ and $(\omega^*_{\rm m},\ \tau^*_{\rm m})$ of the engine and motor, respectively, which can improve energy conservation, and the battery SOC can be managed in the proper range. Note from the relation (42) that the driving torque demand $\tau^*_{\rm dr}$ can be determined with v^*. Subsequently, owing to the relations (37) and (38), it has two degrees of freedom to deal with the power distribution between the engine and motor in the HEV operating mode. In this study, we selected $u = [\omega^*_{\rm e},\ \tau^*_{\rm e}]^\top$ as the design variable. Furthermore, the power distribution problem should be solved when the vehicle is in the HEV operating mode. To simplify the design, we consider that during the driving stage, the operating mode is decided according to the following rule:

$$\begin{cases} \text{HEV mode}, & \dfrac{1}{R_{\rm tire}}\tau^*_{\rm dr} v^* \geqslant P^0_{\rm dr}, \\ \text{EV mode}, & \text{others}, \end{cases} \tag{45}$$

where $P^0_{\rm dr}$ denotes a given small constant.

Finally, for a $v^*(t_k)$, $k = 0, 1, \ldots, T$ with the corresponding $\tau^*_{\rm dr}$, the power distribution of the HEV powertrain system can be formulated as an optimal control problem with both the equality and inequality constraints, that is,

$$\min_{u(t_k)} J({\rm SOC}_0) = \sum_{k=0}^{T-1}\Big[r_{\rm f} \cdot m_{\rm f}(u(t_k)) \cdot \Delta t + r_{\rm e} \cdot \big({\rm SOC}(t_k) - {\rm SOC}_{\rm ref}\big)^2\Big] \tag{46a}$$

subject to

$$\begin{cases} {\rm SOC}(t_{k+1}) = f\big({\rm SOC}(t_k), \tau_{\rm m}(v^*(t_k), \tau^*_{\rm e}(t_k)), \omega_{\rm m}(\omega^*_{\rm e}(t_k))\big), \quad {\rm SOC}(0) = {\rm SOC}_0, \\ {\rm SOC}_{\rm m} \leqslant {\rm SOC}(t_k) \leqslant {\rm SOC}_{\rm M}, \\ \tau_{\rm em} \leqslant \tau^*_{\rm e}(t_k) \leqslant \tau_{\rm eM}(\omega^*_{\rm e}(t_k)), \\ \omega_{\rm em}(v^*(t_k), i_{\rm gm}) \leqslant \omega^*_{\rm e}(t_k) \leqslant \omega_{\rm eM}(v^*(t_k), i_{\rm gM}), \end{cases} \tag{46b}$$

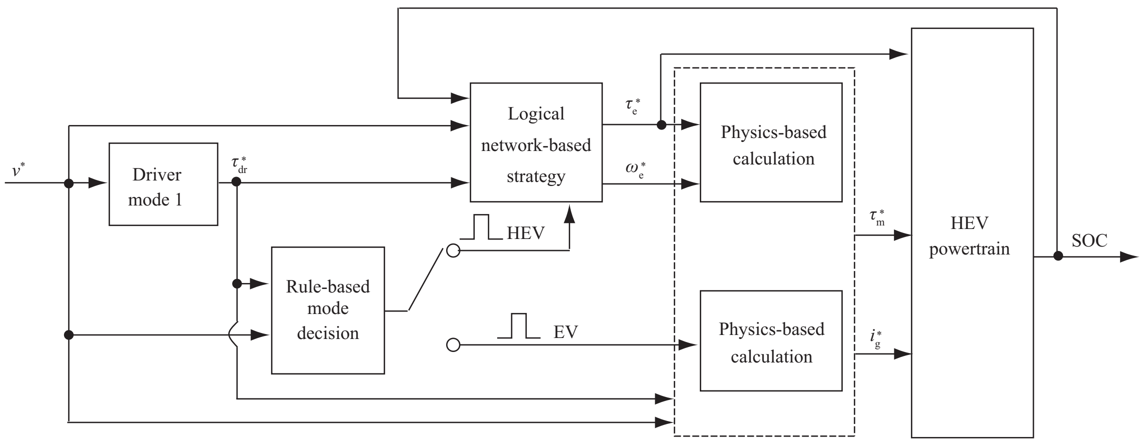

Figure 3 Design framework of the HEV energy management problem.

where $m_{\rm f}$ denotes the fuel mass flow rate, which is an identified polynomial of the $\omega_{\rm e}$ and $\tau_{\rm e}$, $r_{\rm f}$ and $r_{\rm e}$ are the weighting factors, $\text{SOC}_{\rm m}$ and $\text{SOC}_{\rm M}$ are the upper and lower bound of SOC, $\tau_{\rm em}$, $\tau_{\rm eM}$, $\omega_{\rm em}$, $\omega_{\rm eM}$, $i_{\rm gm}$ and $i_{\rm gM}$ are the corresponding limiting values, and $\text{SOC}_{\rm ref}$ is the target SOC value. Note that the target $\text{SOC}_{\rm ref}$ denotes the final SOC value of the HEV battery [8]; in this study, it is considered to be constant, that is, $\text{SOC}_{\rm ref} = 0.5$. The $\omega_{\rm em}$ and $\omega_{\rm eM}$ were calculated according to relation (38). Problem (46) is a nonlinear, constrained optimal control problem.

Finally, for the considered HEV system, expect for $\tau_{\rm e}^*$, the motor torque demand $\tau_{\rm m}^*$ and desired gear ratio $i_{\rm g}^*$ are also real input variables. The following shows how to obtain the two variables based on the physics-based relations (37) and (38), as well as the obtained optimal solution $(\omega_{\rm e}^*, \tau_{\rm e}^*)$. First, during the HEV mode, the desired gear ratio $i_{\rm g}^*$ can be obtained as follows:

$$i_{\rm g}^*(t_k) = \frac{R_{\rm tire}}{i_0 v^*(t_k)} \omega_{\rm e}^*(t_k), \tag{47}$$

and the motor torque demand $\tau_{\rm m}^*$ can be calculated according to the following relation:

$$\tau_{\rm m}^*(t_k) = \frac{\tau_{\rm dr}^*(t_k)}{i_{\rm g}^*(t_k) i_0 \eta_{\rm f}} - \tau_{\rm e}^*(t_k). \tag{48}$$

In the EV mode, suppose that the desired gear ratio is set as $i_{\rm g}^*(t_k) = i_{\rm gM}$, and the motor torque demand $\tau_{\rm m}^*(t_k)$ can also be calculated using (48) with $\tau_{\rm e}^*(t_k) = 0$. Finally, Figure 3 shows a block diagram of the proposed energy management scheme.

4.2 HEV problem solution

The formulated problem (46) is solved by applying the deduced Algorithm 1. Select $r_{\rm f} = 1$, $r_{\rm e} = 800$, $\Delta t = 1$ s, and $P_{\rm dr}^0 = 1000$. The test scenario is illustrated in Figure 4, which differs from the Worldwide Harmonized Light Vehicles Test Procedure (WLTP) cycle developed by the European Union [40]. The testing route is shown in Figure 4 where the horizon $T = 200$. Furthermore, for the control design, the ranges of the state and two control variables are set as follows:

$$0.4 \leqslant \text{SOC} \leqslant 0.6, \quad 1000 \text{ r} \cdot \text{min}^{-1} \leqslant \omega_{\rm e} \leqslant 4500 \text{ r} \cdot \text{min}^{-1}, \quad 10 \text{ N} \cdot \text{m} \leqslant \tau_{\rm e} \leqslant 150 \text{ N} \cdot \text{m}. \tag{49}$$

For evaluation, the results of 128 cases are presented with respect to different quantification indices $n_x \in [3:1:10]$ and $n_{u1} = n_{u2} \in [2:1:5]$. The corresponding quantitative values $D_{\rm SOC}$, $D_{\omega e}$ and $D_{\tau e}$ with respect to the SOC, $\omega_{\rm e}$ and $\tau_{\rm e}$ are shown in Table 2.

Remark 3. It should be noted from constraints (46b) that the control variables $\omega_{\rm e}^*$ and $\tau_{\rm e}^*$ are dependent on the other boundary values of the system; in other words, not all quantitative control variables are feasible. Hence, the feasible region is first determined at each step.

The obtained solutions were evaluated using a constructed HEV simulator according to the industrial vehicle parameters. First, we choose the initial condition as $\text{SOC}_0 = 0.55$. Figure 5 presents the total

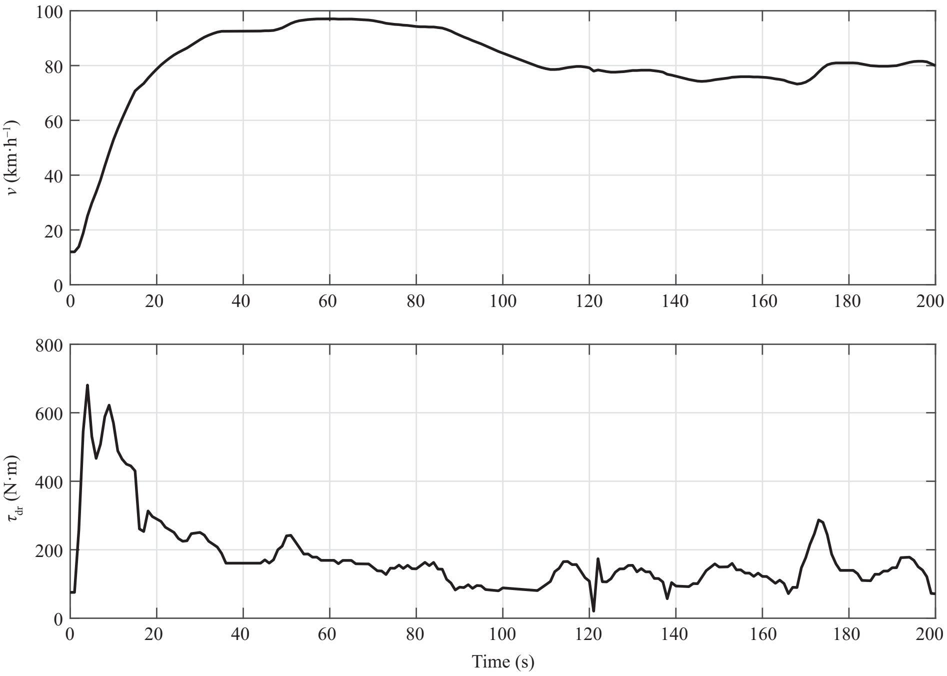

Figure 4 Testing scenario data: vehicle speed trajectory and driving torque demand.

Table 2 Selected quantitative values

Parameter	Value
D_{SOC}	$\{2.5,\ 1.25,\ 0.62,\ 0.31,\ 0.16,\ 0.08,\ 0.04,\ 0.02\ \}\times10^{-2}$
$D_{\omega e}$	$\{875,\ 438,\ 219,\ 109\ \}\ \mathrm{r}\cdot\mathrm{min}^{-1}$
$D_{\tau e}$	$\{35,\ 17.5,\ 8.8,\ 4.4\ \}\ \mathrm{N}\cdot\mathrm{m}$

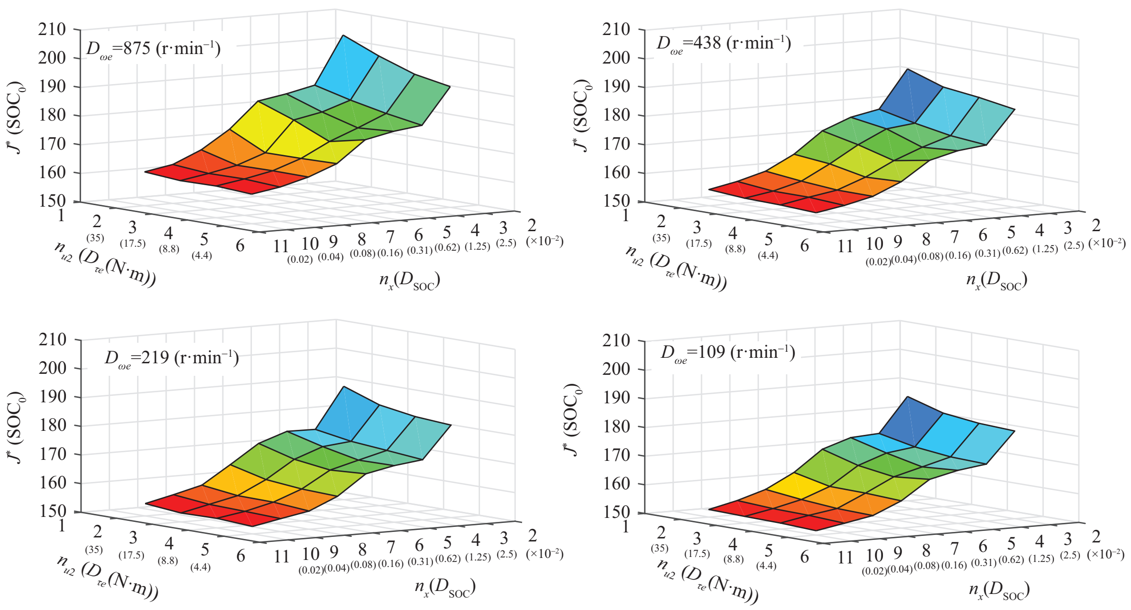

Figure 5 (Color online) Total cost of each case (each point in the grid shows one solution with respect to different $D_{\tau e}$, D_{SOC}, and $D_{\omega e}$).

costs $J^*(\mathrm{SOC}_0)$ for the 128 cases. Because the problem solution relates to three quantitative variables, that is, D_{SOC}, $D_{\omega e}$ and $D_{\tau e}$, the results shown in Figure 5 are divided into four subfigures, and each subfigure shows the corresponding 32 solutions with respect to one of the four $D_{\omega e}$. It can be observed from this figure that the cost is decreased when the quantitative factors of the state and control variables

Table 3 Performance results of 8 cases

$D_{\omega e}$ ($\mathrm{r \cdot min^{-1}}$)	$D_{\tau e}$ ($\mathrm{N \cdot m}$)	D_{SOC}	Fuel (L)	Electricity (kWh)	Cost	Computation time (s)
875	35	2.5	0.19	0.23	203.9	0.55
		0.02	0.15	0.38	161.8	69.01
	4.4	2.5	0.17	0.24	186.4	2.71
		0.02	0.14	0.39	152.7	395.49
109	35	2.5	0.18	0.24	192.1	2.61
		0.02	0.15	0.38	160.3	384.41
	4.4	2.5	0.17	0.25	180.6	16.95
		0.02	0.14	0.38	151.5	2369.69

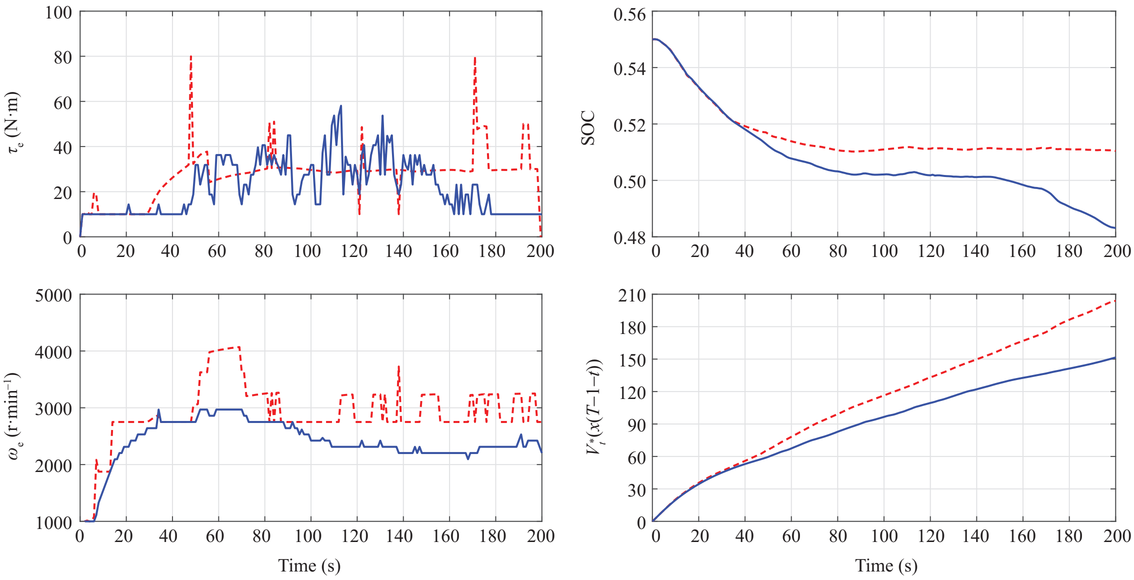

Figure 6 (Color online) Results of 2 cases by the logical control strategy (dashed line: $D_{\mathrm{SOC}} = 2.5 \times 10^{-2}$, $D_{\omega e} = 875$ $\mathrm{r \cdot min^{-1}}$, $D_{\tau e} = 35$ $\mathrm{N \cdot m}$; solid line: $D_{\mathrm{SOC}} = 0.02 \times 10^{-2}$, $D_{\omega e} = 109$ $\mathrm{r \cdot min^{-1}}$, $D_{\tau e} = 4.4$ $\mathrm{N \cdot m}$)

are small. Moreover, it should be noted that for any quantitative selection of the control variables, when $D_{\mathrm{SOC}} \leqslant 0.04 \times 10^{-2}$, the cost decrement is small. Table 3 shows the performance results, which are 8 selected cases from all the conducted results. It can be found that with respect to the same $D_{\tau e}$ and $D_{\omega e}$, the total cost can be reduced more than 18%, and the most fuel economy can achieve 21% due to the selection of D_{SOC}. However, for the same D_{SOC}, the selection on $D_{\tau e}$ and $D_{\omega e}$ can mostly improve the cost by 5%. However, the computation time increases considerably as using small quantitative factors. Figure 6 shows the curves of the two cases with the maximum and minimum quantitative factors of both the state and control variables. It can be observed that large $D_{\tau e}$ and $D_{\omega e}$ can lead obvious changes on the desired engine operating point, and this phenomenon has unexpected influence to the actuators of the engine system in practice. Hence, the selection of proper quantitative factors should consider the tread-off between computation time, cost performance and the management of the transient control variables.

Because the HEV energy management problem is formulated as a nonlinear optimal control problem, an analytical solution cannot be obtained. Despite this, the obtained results verify that in a DP-based algorithm, the quantification for both the state variables and control inputs has a significant influence on the performance of a control problem. In other words, the presented result in Theorem 2 is significant, as it provides a theoretical basis for the selection of proper quantitative factors.

Furthermore, to evaluate the dependence of the initial state value on the solution, ten solutions were extracted with respect to different SOC_0 ($= 0.4, 0.42, \ldots, 0.6$). The results are shown in Figure 7. The obtained solutions guarantee the constraints in (46b), and for any SOC_0, the SOC is approximately regulated to $\mathrm{SOC}_{\mathrm{ref}}$. Moreover, it can be observed that when SOC_0 is close to $\mathrm{SOC}_{\mathrm{ref}}$, the engine works as the main power source; otherwise, the motor supplies the most demand power.

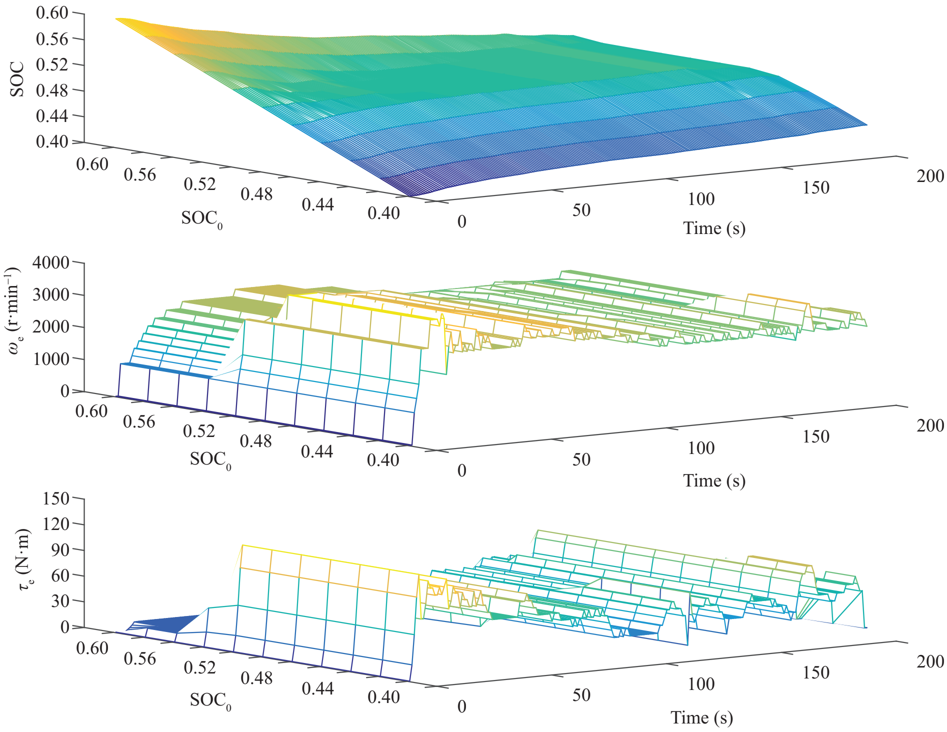

Figure 7 (Color online) State trajectories and solutions under different initial state values: $D_{\rm SOC} = 0.31 \times 10^{-2}$, $D_{\tau e} = 8.8$, $D_{\omega e} = 219$.

5 Conclusion

Since the analytical optimal solutions of discrete-time dynamical systems defined in a continuous domain cannot be obtained, an approximate optimal control design approach is developed in this study. Specifically, by quantifying the system states and control variables, the original optimal control design problem defined in the continuous domain is converted to the one defined in the discrete-time domain. Under suitable assumptions, convergence analysis of the approximate optimal cost with respect to the quantified system and the optimal cost of the original system is established. Furthermore, it was shown that the approximate optimal control problem can be solved using the STP tool. The obtained solutions of the numerical example confirm the convergence to the analytical solution. The effectiveness of the proposed scheme was further evaluated by applying it to solve the energy management optimal control problem of the HEV powertrain system.

Acknowledgements This work was supported in part by National Natural Science Foundation of China (Grant Nos. 62173062, 61973053, 61773090).

References

1 Eriksson L, Nielsen L. Modeling and Control of Engines and Drivelines. Hoboken: John Wiley & Sons, 2014

2 Zhang J, Shen T, Kako J. Short-term optimal energy management of power-split hybrid electric vehicles under velocity tracking control. IEEE Trans Veh Technol, 2020, 69: 182–193

3 Bock H G, Plitt K J. A multiple shooting algorithm for direct solution of optimal control problems. IFAC Proc Vol, 1984, 17: 1603–1608

4 Banks S P, Dinesh K. Approximate optimal control and stability of nonlinear finite-and infinite-dimensional systems. Ann Oper Res, 2000, 98: 19–44

5 Delprat S, Lauber J, Guerra T M, et al. Control of a parallel hybrid powertrain: optimal control. IEEE Trans Veh Technol, 2004, 53: 872–881

6 Serrao L, Onori S, Rizzoni G. A comparative analysis of energy management strategies for hybrid electric vehicles. J Dynamic Syst Measurement Control, 2011, 133: 031012

7 Martinez C M, Hu X, Cao D, et al. Energy management in plug-in hybrid electric vehicles: recent progress and a connected vehicles perspective. IEEE Trans Veh Technol, 2016, 66: 4534–4549

8 Yang Y, Hu X, Pei H, et al. Comparison of power-split and parallel hybrid powertrain architectures with a single electric machine: dynamic programming approach. Appl Energy, 2016, 168: 683–690

9 Wang R, Lukic S M. Dynamic programming technique in hybrid electric vehicle optimization. In: Proceedings of IEEE International Electric Vehicle Conference (IEVC), 2012. 1–8

10 Tang L, Rizzoni G, Lukas M. Comparison of dynamic programming-based energy management strategies including battery life optimization. In: Proceedings of International Conference on Electrical Systems for Aircraft, Railway, Ship Propulsion

and Road Vehicles & International Transportation Electrification Conference (ESARS-ITEC), 2016. 1–6
11 Koot M, Kessels J T B A, de Jager B, et al. Energy management strategies for vehicular electric power systems. IEEE Trans Veh Technol, 2005, 54: 771–782
12 Chen Z, Mi C C, Xu J, et al. Energy management for a power-split plug-in hybrid electric vehicle based on dynamic programming and neural networks. IEEE Trans Veh Technol, 2014, 63: 1567–1580
13 Yang Y, Pei H, Hu X, et al. Fuel economy optimization of power split hybrid vehicles: a rapid dynamic programming approach. Energy, 2019, 166: 929–938
14 Pei D, Leamy M J. Dynamic programming-informed equivalent cost minimization control strategies for hybrid-electric vehicles. J Dyn Syst Meas Control, 2013, 135: 051013
15 Larsson V, Johannesson L, Egardt B. Analytic solutions to the dynamic programming subproblem in hybrid vehicle energy management. IEEE Trans Veh Technol, 2014, 64: 1458–1467
16 Kauffman S A. Metabolic stability and epigenesis in randomly constructed genetic nets. J Theor Biol, 1969, 22: 437–467
17 Truemper K, Truemper K. Design of Logic-based Intelligent Systems. Hoboken: John Wiley & Sons, 2004
18 Cheng D, Qi H. A linear representation of dynamics of boolean networks. IEEE Trans Automat Contr, 2010, 55: 2251–2258
19 Lu J Q, Li B W, Zhong J. A novel synthesis method for reliable feedback shift registers via Boolean networks. Sci China Inf Sci, 2021, 64: 152207
20 Yerudkar A, Del Vecchio C, Glielmo L. Feedback stabilization control design for switched Boolean control networks. Automatica, 2020, 116: 108934
21 Zheng Y T, Li H T, Feng J E. State-feedback set stabilization of logical control networks with state-dependent delay. Sci China Inf Sci, 2021, 64: 169203
22 Li H, Ding X. A control Lyapunov function approach to feedback stabilization of logical control networks. SIAM J Control Optim, 2019, 57: 810–831
23 Zhu S Y, Liu Y, Lou Y J, et al. Stabilization of logical control networks: an event-triggered control approach. Sci China Inf Sci, 2020, 63: 112203
24 Liu Y, Cao J D, Wang L Q, et al. On pinning reachability of probabilistic Boolean control networks. Sci China Inf Sci, 2020, 63: 169201
25 Chen H, Wang Z, Shen B, et al. Model evaluation of the stochastic Boolean control networks. IEEE Trans Automat Contr, 2022, 67: 4146–4153
26 Pal R, Datta A, Dougherty E R. Optimal infinite-horizon control for probabilistic Boolean networks. IEEE Trans Signal Process, 2006, 54: 2375–2387
27 Liu Q, Guo X, Zhou T. Optimal control for probabilistic Boolean networks. IET Syst Biol, 2010, 4: 99–107
28 Toyoda M, Wu Y. On optimal time-varying feedback controllability for probabilistic Boolean control networks. IEEE Trans Neural Netw Learn Syst, 2020, 31: 2202–2208
29 Wu Y, Shen T. An algebraic expression of finite horizon optimal control algorithm for stochastic logical dynamical systems. Syst Control Lett, 2015, 82: 108–114
30 Wu Y, Sun X M, Zhao X, et al. Optimal control of Boolean control networks with average cost: a policy iteration approach. Automatica, 2019, 100: 378–387
31 Wu Y, Guo Y, Toyoda M. Policy iteration approach to the infinite horizon average optimal control of probabilistic Boolean networks. IEEE Trans Neural Netw Learn Syst, 2020, 32: 2910–2924
32 Wu Y, Kumar M, Shen T. A stochastic logical system approach to model and optimal control of cyclic variation of residual gas fraction in combustion engines. Appl Thermal Eng, 2016, 93: 251–259
33 Zhang J Y, Wu Y H. A stochastic logical model-based approximate solution for energy management problem of HEVs. Sci China Inf Sci, 2018, 61: 070207
34 Papagiannis G, Moschoyiannis S. Deep reinforcement learning for control of probabilistic boolean networks. In: Proceedings of International Conference on Complex Networks and Their Applications. Berlin: Springer, 2020. 361–371
35 Teo K L, Li B, Yu C, et al. Applied and computational optimal control: a control parametrization approach. In: Springer Optimization and Its Applications. Berlin: Springer, 2021
36 Goh C J, Teo K L. Control parametrization: a unified approach to optimal control problems with general constraints. Automatica, 1988, 24: 3–18
37 Zhang J, Wu Y, Shen T. Logical network-based approximate solution of hev energy management problems. In: Proceedings of the 46th Annual Conference of the IEEE Industrial Electronics Society, 2020. 2044–2049
38 Cheng D, Qi H, Li Z. Analysis and Control of Boolean Networks: A Semi-Tensor Product Approach. Berlin: Springer, 2011
39 Kirk D E. Optimal Control Theory: An Introduction. New York: Dover Publications, 2004
40 Mock P, Kühlwein J, Tietge U, et al. The WLTP: how a new test procedure for cars will affect fuel consumption values in the EU. Int Council Clean Trans, 2014, 9: 35–47

Appendix A

Proof of Lemma 1. We prove estimation (8) using induction. For $t = 1$, the estimation (8) holds because

$$\begin{aligned} |x(1; f, x_0, \boldsymbol{u}) - x(1; f, y_0, \boldsymbol{v})| &= |f(x_0, u(0)) - f(y_0, v(0))| \\ &\leqslant k_f(|x_0 - y_0| + |u(0) - v(0)|) \\ &\leqslant k_f(|x_0 - y_0| + \|\boldsymbol{u} - \boldsymbol{v}\|), \end{aligned}$$

using the Lipschitz assumption (C1) on f and the definition of norm $\|\cdot\|$ in $\mathcal{U}$, as given in (11). We assume that the estimation (8) holds for $t-1$; that is,

$$|x(t-1; f, x_0, \boldsymbol{u}) - x(t-1; f, y_0, \boldsymbol{v})| \leqslant k_f^{t-1}|x_0 - y_0| + K_1(t-1)\|\boldsymbol{u} - \boldsymbol{v}\|. \tag{A1}$$

Then, according to assumption (C1) and inequality (A1), we obtain

$$\begin{aligned} |x(t; f, x_0, \boldsymbol{u}) - x(t; f, y_0, \boldsymbol{v})| &= |f(x(t-1), u(t-1)) - f(y(t-1), v(t-1))| \\ &\leqslant k_f(|x(t-1) - y(t-1)| + |u(t-1) - v(t-1)|) \end{aligned}$$

$$\leqslant k_f^t|x_0-y_0|+(K_1(t-1)+k_f)\|\boldsymbol{u}-\boldsymbol{v}\|), \tag{A2}$$

where $x(t-1)$ and $y(t-1)$ denote $x(t-1;f,x_0,\boldsymbol{u})$ and $x(t-1;f,y_0,\boldsymbol{v})$, respectively. Thus, noting that $k_f(K_1(t-1)+1)=K_1(t)$ and by the definition of $K_1(\cdot)$ given in (10), we prove condition (8). Furthermore, by applying assumption (C2), we obtain

$$\begin{aligned}|J(f,x_0,\boldsymbol{u})-J(f,y_0,\boldsymbol{v})| &\leqslant k_h|x(T;f,x_0,\boldsymbol{u})-x(T;f,y_0,\boldsymbol{v})|+\sum_{t=1}^{T-1}k_g|x(t;f,x_0,\boldsymbol{u})-x(t;f,y_0,\boldsymbol{v})|\\ &\leqslant k_hk_f^{\top}|x_0-y_0|+k_hK_1(T)\|\boldsymbol{u}-\boldsymbol{v}\|+\sum_{t=1}^{T-1}k_g(k_f^t|x_0-y_0|+K_1(t)\|\boldsymbol{u}-\boldsymbol{v})\\ &= K_2|x_0-y_0|+K_3\|\boldsymbol{u}-\boldsymbol{v}\|,\end{aligned}$$

where estimation (8) is used in the second inequality and we complete the proof of estimation (9).

Proof of Theorem 1. As defined in problem (P), let $\boldsymbol{u}_{f,x_0}$ and $\boldsymbol{u}_{f,y_0}$ be the optimal control inputs corresponding to $J^*(f,x_0)$ and $J^*(f,y_0)$, respectively; that is, $J(f,x_0,\boldsymbol{u}_{f,x_0})=J^*(f,x_0)$ and $J(f,y_0,\boldsymbol{u}_{f,y_0})=J^*(f,y_0)$. Then, according to the estimation (9) of Lemma 1,

$$|J(f,y_0,\boldsymbol{u}_{f,x_0})-J^*(f,x_0)|=|J(f,y_0,\boldsymbol{u}_{f,x_0})-J(f,x_0,\boldsymbol{u}_{f,x_0})|<K_2|x_0-y_0|, \tag{A3}$$

$$|J(f,x_0,\boldsymbol{u}_{f,y_0})-J^*(f,y_0)|=|J(f,x_0,\boldsymbol{u}_{f,y_0})-J(f,y_0,\boldsymbol{u}_{f,y_0})|<K_2|x_0-y_0|. \tag{A4}$$

By noting that $J^*(f,y_0)\leqslant J(f,y_0,\boldsymbol{u}_{f,x_0})$, it follows from (A3) that

$$J^*(f,y_0)-J^*(f,x_0)\leqslant J(f,y_0,\boldsymbol{u}_{f,x_0})-J^*(f,x_0)<K_2|x_0-y_0|. \tag{A5}$$

Similarly, from the inequality $J^*(f,x_0)\leqslant J(f,x_0,\boldsymbol{u}_{f,y_0})$ and (A4), the following condition holds:

$$J^*(f,x_0)-J^*(f,y_0)\leqslant J(f,x_0,\boldsymbol{u}_{f,y_0})-J^*(f,y_0)<K_2|x_0-y_0|. \tag{A6}$$

Combining (A5) and (A6), we obtain (12).

Proof of Proposition 2. Recall that for all $x\in X, u\in U$, we have $|q_n(x)-x|\leqslant\|\mathscr{S}_n\|$ and $|q_m(u)-u|\leqslant\|\mathscr{E}_m\|$, as given in (19). Hence, by definition (20) of quantification operator $\hat{f}_m^n$, we have that

$$\begin{aligned}\left|\hat{f}_m^n(x,u)-f(x,u)\right| &\leqslant |q_n(f(x,q_m(u)))-f(x,q_m(u))|+|f(x,q_m(u))-f(x,u)|\\ &\leqslant k_f|q_m(u)-u|+\|\mathscr{S}_n\|\\ &\leqslant k_f\|\mathscr{E}_m\|+\|\mathscr{S}_n\|,\end{aligned} \tag{A7}$$

and prove (21).

Proof of Lemma 2. The induction technique is also used to prove (24). For $t=1$, recalling Definition 4 for the quantification function $\hat{f}_m^n$, we have

$$\begin{aligned}|\hat{x}_n(1)-x(1)| &= \left|\hat{f}_m^n(q_n(x_0),q_m(u(0)))-f(x(0),u(0))\right| \\ &\leqslant \left|\hat{f}_m^n(q_n(x_0),q_m(u(0)))-f(q_n(x_0),q_m(u(0)))\right|+|f(q_n(x_0),q_m(u(0)))-f(x(0),u(0))|.\end{aligned} \tag{A8}$$

Hence, according to Proposition 2 and assumption (C1), we obtain

$$\begin{aligned}|\hat{x}_n(1)-x_n(1)| &\leqslant \|\mathscr{S}_n\|+k_f\|\mathscr{E}_m\|+k_f(\|\mathscr{S}_n\|+\|\mathscr{E}_m\|)\\ &=(k_f+1)\|\mathscr{S}_n\|+2k_f\|\mathscr{E}_m\|.\end{aligned} \tag{A9}$$

This implies that the condition (24) holds for $t=1$. Now, we assume that Eq. (24) holds for $t-1$, that is,

$$|\hat{x}_n(t-1)-x(t-1)|\leqslant(K_1(t)/k_f)\|\mathscr{S}_n\|+K_1(t-1)\|\mathscr{E}_m\|. \tag{A10}$$

Then, for t, we have

$$\begin{aligned}|\hat{x}_n(t)-x_n(t)| &= \left|\hat{f}_m^n(\hat{x}_n(t-1),q_m(u(t-1)))-f(x(t-1),u(t-1))\right|\\ &\leqslant \left|\hat{f}_m^n(\hat{x}_n(t-1),q_m(u(t-1)))-f(\hat{x}_n(t-1),q_m(u(t-1)))\right|\\ &\quad+|f(\hat{x}_n(t-1),q_m(u(t-1)))-f(x(0),u(0))|\\ &\leqslant \|\mathscr{S}_n\|+k_f\|\mathscr{E}_m\|+k_f(|\hat{x}_n(t-1)-x(t-1)|+|q_m(u(t-1))-u(t-1)|),\end{aligned}$$

using Proposition 2 and assumption (C1). Furthermore, assumption condition (A10) implies that

$$\begin{aligned}|\hat{x}_n(t)-x_n(t)| &\leqslant \|\mathscr{S}_n\|+2k_f\|\mathscr{E}_m\|+k_f\left(K_1(t)/k_f\|\mathscr{S}_n\|+K_1(t-1)\|\mathscr{E}_m\|\right)\\ &= (K_1(t+1)/k_f)\|\mathscr{S}_n\|+K_1(t)\|\mathscr{E}_m\|.\end{aligned}$$

The proof of Lemma 2 is completed.

Proof of Lemma 3. Recalling the definition of the cost function (3), (5) and (6) in assumption (C2), we obtain

$$|J(f,x_0,\boldsymbol{u})-J(\hat{f}_m^n,x_0,\boldsymbol{u})| \leqslant k_h|x(T;f,x_0,\boldsymbol{u})-\hat{x}(T;\hat{f}_m^n,x_0,\boldsymbol{u})| \tag{A11}$$

$$+\sum_{t=1}^{T-1} k_g|x(t;f,x_0,\boldsymbol{u})-\hat{x}(t;\hat{f}_m^n,x_0,\boldsymbol{u})|.$$

Then, applying Lemma 2, we obtain inequality (25). Furthermore, because $q_m(\boldsymbol{u})=\boldsymbol{u}$, when $\boldsymbol{u}\in\mathcal{U}_m$, we obtain the second estimation (26).

Proof of Theorem 2. Recall that $\boldsymbol{u}_{f,x_0}$ and $\boldsymbol{u}_{\hat{f}_m^n,x_0}$ correspond to the optimal control inputs of problem (P) and approximate problem $(\mathrm{AP})_m^n$, respectively; that is,

$$\begin{aligned}&J(f,x_0,\boldsymbol{u}_{f,x_0})=J^*(f,x_0),\\&J(\hat{f}_m^n,q_n(x_0),\boldsymbol{u}_{\hat{f}_m^n,x_0})=J^*(\hat{f}_m^n,x_0).\end{aligned}\tag{A12}$$

It is obvious that

$$J^*(f,x_0)\leqslant J(f,x_0,\boldsymbol{u}_{\hat{f}_m^n,x_0}),\tag{A13}$$

since $\mathcal{U}_m\subset\mathcal{U}$. Furthermore, by (26) of Lemma 3 and noting that $\boldsymbol{u}_{\hat{f}_m^n,x_0}$ is the optimal control of the approximate problem $(\mathrm{AP})_m^n$, that is, $J(\hat{f}_m^n,q_n(x_0),\boldsymbol{u}_{\hat{f}_m^n,x_0})=J^*(\hat{f}_m^n,x_0)$, we obtain

$$\begin{aligned}\left|J(f,x_0,\boldsymbol{u}_{\hat{f}_m^n,x_0})-J^*(\hat{fx}_m^n,x_0)\right| &= \left|J(f,x_0,\boldsymbol{u}_{\hat{f}_m^n,x_0})-J(\hat{f}_m^n,x_0,\boldsymbol{u}_{\hat{f}_m^n,x_0})\right|\\&\leqslant K_4\|\mathscr{S}_n\|.\end{aligned}\tag{A14}$$

Combining the above two inequalities (A13) and (A14), we have

$$J^*(f,x_0)-J^*(\hat{f}_m^n,x_0)\leqslant K_4\|\mathscr{S}_n\|.\tag{A15}$$

Let

$$q_m(\boldsymbol{u}_{f,q_n(x_0)}):=\left\{q_m(u^*_{f,q_n(x_0)}(t)):0\leqslant t\leqslant T-1\right\},\tag{A16}$$

where $\boldsymbol{u}_{f,q_n(x_0)}=\{u^*_{f,q_n(x_0)}(t)):0\leqslant t\leqslant T-1\}$ is the corresponding optimal control input of problem (P) with initial state $x(0)=q_n(x_0)$. Then, according to Theorem 1 and inequality (19), we have

$$\left|J^*(f,x_0)-J(f,x_0,\boldsymbol{u}_{f,q_n(x_0)})\right|\leqslant K_2\|\mathscr{S}_n\|,$$

which implies that

$$\begin{aligned}\left|J(\hat{f}_m^n,x_0,q_m(\boldsymbol{u}_{f,q_n(x_0)}))-J^*(f,x_0)\right| &\leqslant K_2\|\mathscr{S}_n\|+\left|J(\hat{f}_m^n,x_0,q_m(\boldsymbol{u}_{f,q_n(x_0)}))-J(f,x_0,q_m(\boldsymbol{u}_{f,q_n(x_0)}))\right|\\&\quad+\left|J(f,x_0,q_m(\boldsymbol{u}_{f,q_n(x_0)})-J(f,x_0,\boldsymbol{u}_{f,q_n(x_0)})\right|.\end{aligned}$$

Applying Lemma 3 and condition (9) of Lemma 1 to the inequality above, we obtain

$$\begin{aligned}\left|J(\hat{f}_m^n,x_0,q_m(\boldsymbol{u}_{f,q_n(x_0)}))-J^*(f,x_0)\right| &\leqslant (K_4+K_2)\|\mathscr{S}_n\|+K_5\|\mathscr{E}_m\|+K_3\|\boldsymbol{u}_{f,q_n(x_0)}-q_m(\boldsymbol{u}_{f,q_n(x_0)})\|\\&\leqslant (K_4+K_2)\|\mathscr{S}_n\|+(K_5+K_3)\|\mathscr{E}_m\|.\end{aligned}\tag{A17}$$

Furthermore, as $q_m(\boldsymbol{u}_{f,q_n(x_0)})\in\mathcal{U}_m$, we have

$$J^*(\hat{f}_m^n,x_0)\leqslant J(\hat{f}_m^n,x_0,q_m(\boldsymbol{u}_{f,q_n(x_0)})).$$

Therefore, by (A17), we obtain

$$J^*(\hat{f}_m^n,x_0)-J^*(f,x_0)\leqslant(K_2+K_4)\|\mathscr{S}_n\|+(K_3+K_5)\|\mathscr{E}_m\|.\tag{A18}$$

Finally, by combining (A15) and (A18), we obtain error estimation (28).